HHS Public Access

Author manuscript

Biochemistry. Author manuscript; available in PMC 2023 June 23.

Published in final edited form as:

Biochemistry. 2022 September 06; 61(17): 1766–1773. doi:10.1021/acs.biochem.2c00283.

Untwisted α-synuclein Filaments formed in the Presence of Lipid Vesicles

Anvesh K. R. Dasari[1], **Lucas Dillard**[2], **Sujung Yi**[1], **Elizabeth Viverette**[2], **Alimohammad Hojjatian**[3], **Urmi Sengupta**[4], **Rakez Kayed**[4], **Kenneth A. Taylor**[3], **Mario J. Borgnia**[2], **Kwang Hun Lim**[1,*]

[1]Department of Chemistry, East Carolina University, Greenville, NC 27858, USA.

[2]Genome Integrity and Structural Biology Laboratory, National Institute of Environmental Health Sciences, National Institutes of Health, Department of Health and Human Services, Research Triangle Park, NC, 27709, USA.

[3]Institute of Molecular Biophysics, Florida State University, Tallahassee, FL 32306-4380, USA.

[4]Departments of Neurology, Neuroscience and Cell Biology, University of Texas Medical Branch, Galveston, TX, 77555, USA.

Abstract

Accumulation of filamentous aggregates of α-synuclein is a pathological hallmark of several neurodegenerative diseases including Parkinson's disease (PD). Interaction between α-synuclein and phospholipids has been shown to play a critical role in the aggregation of α-synuclein. Most structural studies have, however, been focused on α-synuclein filaments formed in the absence of lipids. Here, we report structural investigation of α-synuclein filaments assembled under the quiescent condition in the presence of anionic lipid vesicles using electron microscopy (EM) including cryo-EM. Our transmission electron microscopy (TEM) analyses reveal that α-synuclein forms curly protofilaments at an early stage of aggregation. The flexible protofilaments were then converted to long filaments after a longer incubation of 30 days. More detailed structural analyses using cryo-EM reveal that the long filaments adopt untwisted structures with different diameters, which have not been observed in previous α-synuclein fibrils formed in vitro. The untwisted filaments are rather similar to straight filaments with no observable twist that are extracted from patients with dementia with Lewy bodies. Our structural studies highlight the conformational diversity of α-synuclein filaments, requiring additional structural investigation of not only more ex vivo α-synuclein filaments, but also in vitro α-synuclein filaments formed in the presence of

*Corresponding authors: limk@ecu.edu.

Author Contributions

The manuscript was written through the contributions of all authors. All authors have given approval to the final version of the manuscript.

The authors declare no competing financial interest.

Supporting Information. TEM images of α-synuclein filaments. ThT and ANS binding assays. Cryo-EM structures of WT and G51D α-synuclein fibrils formed in the absence of DMPS vesicles.

Accession Codes

α-synuclein: UniProtKB entry P37840

diverse co-factors to better understand the molecular basis of diverse molecular conformations of α-synuclein filaments.

Graphical Abstract

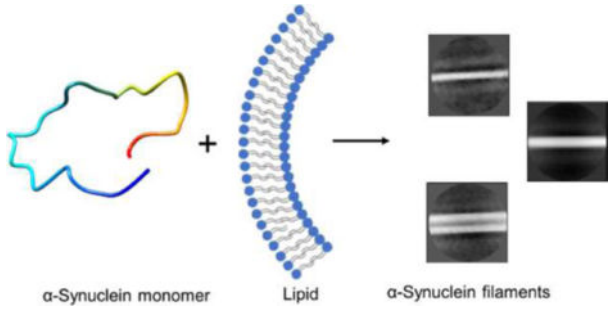

Introduction

Intracellular deposition of misfolded α-synuclein is a hallmark of Parkinson's disease (PD), dementia with Lewy bodies (DLB), and multiple system atrophy (MSA), collectively termed synucleinopathies.[1] Structural characterization of filamentous α-synuclein aggregates is essential to understanding the molecular mechanism of α-synuclein aggregation. Atomic-resolution structures of α-synuclein filaments determined by solid-state NMR and cryo-EM revealed diverse molecular conformations,[2–6] suggesting the presence of multiple misfolding and aggregation pathways. In addition, various pathogenic single-point mutations, including E46K, G51D, and A53T were shown to induce distinct molecular conformations of α-synuclein.[7–10]

Recent structural studies of ex vivo α-synuclein filaments also revealed that α-synuclein filaments extracted from MSA and DLB patients' brains exhibit distinct molecular conformations from those of the in vitro α-synuclein filaments.[11] In particular, filaments derived from DLB patient brains were shown to adopt untwisted fibril morphologies,[11, 12] which have not been observed for in vitro α-synuclein filaments[13]. In addition, our recent structural studies showed that interaction between the microtubule binding protein, tau, and α-synuclein promotes the formation of α-synuclein filaments with distinct conformations.[14, 15] Previous solid-state NMR studies also revealed that α-synuclein filaments derived by anionic phospholipids have distinct molecular conformations in the N-terminal region.[16] These results suggest that cofactors in cellular environments might interact with α-synuclein, leading the protein to a specific misfolding pathway for the formation of distinct α-synuclein filaments.[17, 18]

There is mounting evidence that suggests interactions between α-synuclein and lipid membranes play an important role in misfolding and aggregation of α-synuclein.[19–22] In particular, α-synuclein localized in presynaptic neural terminals was suggested to interact with synaptic lipid vesicles, which is associated with normal function as well as misfolding and aggregation.[23, 24] Lipid vesicles consisting of anionic phospholipids (1,2-dimyristoyl-sn-glycero-3-phospho-L-serine, DMPS) have been used as model membranes since DMPS is a key component of the synaptic vesicles.[19, 25] Previous studies revealed that DMPS

vesicles with a diameter of 20 – 100 nm promote the formation of filamentous aggregates of α-synuclein.[19, 26, 27] In addition, recent high-resolution imaging of Lewy bodies (LB) extracted from PD patients revealed the co-presence of α-synuclein aggregates and lipid-rich inclusions in the LB,[28] supporting the important role of lipids. In this study, structural features of wild-type (WT) α-synuclein filaments in the presence of lipid vesicles (DMPS) were investigated to compare their structural characteristics to those of previously reported in vitro and ex vivo α-synuclein filaments. In addition to WT α-synuclein, a pathogenic variant (G51D) associated with early-onset familial PD[29] was also used to examine the effect of the mutation on the N-terminal region that is responsible for interactions with lipid membranes.[30] Structural and biochemical properties of the two filamentous aggregates derived by the lipid vesicles were compared. The effect of pH on oligomer formation was also investigated since the synaptic vesicles undergo pH changes from 7.4 to 5.5 during their life cycle.[31]

Methods

Materials and Methods

α-synuclein expression and purification—Full-length human α-synuclein plasmid (pET21a, a gift from Michael J Fox Foundation, Addgene plasmid # 51486) was transformed into BL21(DE3) *E. coli* cells and expressed in LB medium as described previously[32]. Briefly, the transformed *E. coli* cells were grown in LB medium containing carbenicillin (100 μg/mL) at 37 ^{O}C. When OD_{600} of cell culture reached 0.8, α-synuclein expression was induced by adding 0.5 mM IPTG. After 12 hours of incubation at 25 ^{O}C, cells were harvested by centrifugation. The resultant cell pellet was sonicated in lysis buffer (20 mM Tris, 150 mM NaCl, pH 8.0), and the soluble fraction of the cell lysate was precipitated with 50 % ammonium sulfate at 4 ^{O}C, then centrifuged. The resultant protein pellet was re-suspended in dialysis buffer (10 mM tris buffer, 2 mM EDTA, pH 8.0) and dialyzed against the same buffer overnight at 4 ^{O}C. α-synuclein was further purified by anion exchange chromatography (HiTrap Q HP; 20 mM tris buffer, pH 8) followed by gel filtration (HiLoad 16/60 Superdex 75 pg) at 4 °C.

Preparation of lipid vesicles

1,2-dimyristoyl-sn-glycero-3-phospho-L-serine (DMPS) lipids were prepared by re-suspending dried DMPS (3 mM) in 10 mM phosphate buffer (pH 6.5) and stirring at 45 ^{O}C for 2 hrs. Lipids were then subjected to 5 freeze/thaw cycles. Lipid vesicles were prepared by extruding the lipid solution 11 times through a 0.1 μm membrane filter at 45 ^{O}C. The average diameter of lipid vesicles was then confirmed using dynamic light scattering measurements.

Dynamic Light Scattering (DLS)

The size distribution of lipid vesicles was measured using DynaPro NanoStar DLS instrument. DMPS lipid vesicles were diluted to 30 μM in 10 mM phosphate buffer (pH 6.5), and a 20 μL of lipid suspension was added to a quartz cuvette. DLS measurements were recorded with an acquisition time of 3 sec and ten repetitions with a laser wavelength of 658 nm.

Preparation of α-synuclein aggregates

Monomeric α-synuclein (60 μM) was incubated in the presence of DMPS (100 μM) at pH 7.4 or 6.5 for three weeks at 37 ^{O}C or 30 ^{O}C under quiescent conditions and filaments were collected by centrifugation. In order to prepare α-synuclein fibrils in the absence of the lipids, α-synuclein (60 μM) was incubated in PBS (10 mM phosphate buffer, 150 mM NaCl, pH 7.4) for one week at 37 ^{O}C and the fibrils were collected by centrifugation.

Aggregation assay

α-synuclein aggregation kinetics were monitored by measuring ThT fluorescence using a SpectraMax® microplate reader. Monomeric α-synuclein (60 μM) was incubated with 50 μM thioflavin T (ThT) in the presence or absence of DMPS lipids (100 μM). A 200 μL of each sample was added in duplicates to a 96 well black clear bottom microplate and sealed airtight. Microplates were incubated at 37 ^{O}C or 30 ^{O}C under quiescent conditions. ThT fluorescence emission was monitored at 482 nm with an excitation of 440 nm.

Negative staining Transmission Electron Microscopy (TEM)

α-synuclein samples (5 μL) incubated in the presence or absence of lipids were added onto a carbon-coated formvar copper 300 mesh grids. After 30 sec of incubation excess sample was blotted off with a filter paper. Grids were then stained with 5 μL of 1% uranyl acetate and incubated for 30 sec. Excess stain was blotted off with filter paper, and grids were allowed to air dry. α-synuclein samples were then imaged under Philips CM12 transmission electron microscope at an accelerating voltage of 80kV.

Cryo-EM sample preparation, data collection, and image processing

A 3 μL of the α-synuclein sample was applied to a glow discharged UltrAuFoil 1.2/1.3 300 mesh grid (Quantifoil) and reverse blotted for 20 sec on a Leica plunge freezing instrument with chamber conditions of 15 °C and 95 % humidity. A total number of 1050 images were collected at a nominal magnification of 45,000X on a 200 kV Talos Arctica equipped with a K2 Summit direct electron detector (Gatan). Movies were collected as a series of 60 frames at a dose rate of 6 e^{-}/Å^{2}/sec over 9 seconds. Beam-induced motion and drift were corrected using MotionCor2.[33] Aligned (non-dose-weighted) integrated micrographs were used for contrast transfer function (CTF) estimation of each micrograph, using GCTF.[34] α-synuclein filaments were manually picked and extracted with different box sizes in Relion 3.1.[35] Reference free 2D classifications were then performed with 50 classes.

Circular dichroism (CD) spectroscopy

CD spectra of α-synuclein filaments and fibrils formed in the presence and absence of DMPS lipids, respectively, were collected at a final monomeric protein concentration of 10 μM. The CD spectra were recorded on a Jasco 815 spectrometer using a 1 mm pathlength quartz cuvette and an average of 30 scans were acquired for each sample.

Thioflavin T (ThT) and 8-anilino-1-naphthalenesulfonic acid (ANS) fluorescence:

DMPS derived α-synuclein filaments (5 μM) were mixed with ThT working solution (50 μM in 10 mM phosphate buffer) or ANS working solution (20 μM in 10 mM phosphate

buffer). ThT fluorescence (λ_{ex} = 440 nm, λ_{em} = 450–600 nm) and ANS fluorescence (λ_{ex} = 350 nm, λ_{em} = 410–570 nm) were measured with 1 mm slit-width.

Proteinase K (PK) digestion

DMPS derived WT and G51D α-synuclein filaments (0.2 mg/mL) were digested with proteinase K (0.5 ng/μL) at 37 ^{O}C for different time intervals (1 min, 10 min, and 20 min). The digestion reactions were quenched with 1 mm phenylmethylsulfonyl fluoride (PMSF). Samples were then loaded with SDS sample buffer and run on 4–12% gradient bis-tris SDS-PAGE gel.

α-synuclein seeding assays

In order to probe the seeding ability of the DMPS derived α-synuclein filaments, WT and G51D α-synuclein monomers (60 μM) were seeded with their respective DMPS derived α-synuclein filaments at a ratio of 100:1 (protein:seed) in the presence of ThT (50 μM) at 37 °C under constant agitation at 250 rpm. Aggregation kinetics were monitored by measuring ThT fluorescence with excitation and emission wavelengths of 440 nm and 482 nm, respectively.

Cell viability assay

Human neuroblastoma SH-SY5Y cells were cultured in DMEM/F12 (1:1) medium with 10% FBS and 1% Pen-Strep at 37°C. Cells were plated in a clear bottom 96-well black plate at a density of 10,000 cells per well and allowed to attach to the surface for one day. α-synuclein samples at concentrations of 10, 20, and 40 μM were added to the cells and incubated for 48 hours at 37°C. The cell medium was replaced by the fresh cell medium and MTT was added to the wells. After 4 hours of incubation, a solubilizing agent (SDS) was added to the wells and incubated at 37°C. After 4 hours of incubation, the absorbance was measured at 570 nm. Duplicates were measured for each sample.

Results

Aggregation kinetics in the presence of DMPS vesicles

Model membrane vesicles consisting of DMPS with a diameter of 20 – 100 nm have previously been used to explore the effect of lipid vesicles on α-synuclein aggregation and morphology of α-synuclein aggregates mainly at pH 6.5 and 30 °C.[19, 27, 36] In this study, additional incubation conditions were used to prepare filamentous aggregates suitable for more detailed molecular structural characterization using cryo-EM. Small unilamellar vesicles (SUV) with an average diameter of 70 nm were prepared from DMPS via extrusion methods (Figure S1). Aggregation kinetics of wild-type (WT) and mutant (G51D) forms of α-synuclein in the presence and absence of the DMPS lipid vesicles were examined at different pH conditions (pH 6.5 and 7.4) using thioflavin T (ThT) fluorescence (Figure 1). The protein aggregation was greatly accelerated in the presence of the DMPS-SUV for both WT (red) and G51D (green) α-synuclein at pH 6.5 under the quiescent condition (Figure 1a), which is consistent with previously reported kinetics monitored at pH 6.5 and 30 °C.[19, 36] In addition, WT synuclein (red and violet) exhibits accelerated aggregation kinetics than the G51D mutant (green and pink) at both 37 and 30 °C, respectively, presumably

due to less favorable interaction between the more negatively charged G51D mutant and negatively charged DMPS lipid vesicles.

The aggregation kinetics were also monitored at the physiological pH of 7.4 (Figure 1b). The DMPS lipid vesicles induced aggregation of WT (red) and G51D mutant (green) α-synuclein at the physiological pH of 7.4 and 37 °C as well (Figure 1b). Aggregation rates of the two α-synuclein were, however, substantially reduced, and α-synuclein aggregates were observed after longer incubation times at pH 7.4.

Structural features of the filaments formed in the presence of DMPS vesicles

Morphological features of the aggregates were examined using transmission electron microscopy (TEM) (Figure 2). After 7 days of incubation, oligomeric species were observed for G51D α-synuclein (60 μM) in the presence of the lipid vesicles (100 μM) at pH 6.5 and 30 °C (Figure 2a). On the other hand, WT α-synuclein forms curly protofilaments under the same condition (Figure 2b). At a higher temperature of 37 °C, the flexible filamentous aggregates were observed for both G51D and WT α-synuclein at pH 6.5 (Figure 2c and 2d, respectively).

The morphology of α-synuclein filaments formed at the physiological pH (7.4) at 37 °C was also investigated by TEM (Figures S2 and S3). The mutant (G51D) filaments appear to be greatly extended at the higher pH (Figure S2). WT α-synuclein filaments also become somewhat more extended after a longer incubation of 38 days, but they still exhibit curly morphological features (Figure S3). Thus, the mutant (G51D) filaments formed at pH 7.4 were chosen for more detailed structural investigation using cryo-EM.

Untwisted G51D filaments

The G51D α-synuclein filaments formed at pH 7.4 and 37 °C in the presence of DMPS SUVs were frozen on a Quantifoil 1.2/1.3 300 mesh grid and images were acquired at 45,000x magnification on a 200 kV Talos Arctica electron microscope equipped with a Gatan K2 Summit direct detection camera. The cryo-EM micrographs reveal the presence of distinct thin and thick α-synuclein filaments with a diameter of 5 – 13 nm (Figure 3), similar to previously observed filaments isolated from MSA brains which had a diameter of 5 – 18 nm[37].

About 250 micrographs were analyzed using Relion reference-free two-dimensional (2D) classification, which reveals the major species of α-synuclein filaments with different thicknesses (Figure 4, Figure S4, and Table S1). The 2D class averages may originate from different orientations of single asymmetric cylindrical filament or different types of filaments. As for the asymmetric cylindrical filament, it is less likely to observe thinner images from the filaments due to the smaller surface area along that orientation. However, the thinner filaments are more frequently observed in the micrographs (Figure 3) and 2D class averages (Table S1), suggesting that α-synuclein forms at least two distinct filaments in the presence of DMPS vesicles.

The thin and thick filaments are stacked along the axis with a spacing of 4.7 Å, determined by the power spectrum (Figure S4). It is interesting to note that the filaments do not

exhibit helical twists that are observed in the previous cryo-EM structures of the in vitro filaments[2–5] (Figure 4, Figure S4, and Table S2). These results suggest that the DMPS vesicles induce the formation of untwisted filaments, which were observed for the ex vivo filamentous aggregates extracted from DLB patients[11].

Structural and biochemical properties of the α-synuclein filaments

Cryo-EM structural studies of the WT α-synuclein filaments formed in the presence of DMPS vesicles were not amenable due to the curly structural features of the filamentous aggregates. Conventional experimental methods were, therefore, used to compare structural features of the DMPS-induced filaments derived from WT and G51D α-synuclein. Circular dichroism (CD) spectroscopy was initially used to investigate the secondary structure of the two filamentous aggregates (Figure 5a). The CD spectra of the G51D (red solid line) filaments revealed a typical CD spectrum with a maximum at ~195 nm and minimum at ~215 nm observed for β-structured amyloid fibrils, which is consistent with the cryo-EM image of the G51D filaments. However, the DMPS-induced filaments appear to have more helical characters (26%) than the G51D fibrils formed in the absence of lipid vesicles (13%) (red dotted line in Figure 5a and Table S3) based on another minimum at ~ 210 nm. The TEM images also revealed highly flexible, curly filaments (Figure 2), suggesting that the DMPS-induced filaments contain more helical regions than the fibrils formed in the absence of lipid vesicles. The two WT and G51D DMPS-induced filamentous aggregates exhibit almost identical spectra (red and black solid lines), suggesting that the DMPS-induced α-synuclein filaments adopt similar secondary structural features (Table S3). The CD structural studies are in line with similar binding properties of the two filaments for the fluorescence probe, ThT, that is known to bind the grooves formed by the cross-β structures of the fibrils (Figure S5 and S6). The filamentous aggregates are also able to accelerate the aggregation process, suggesting that the DMPS-derived filaments can act as seeds for filament formation (Figure 5b).

Protease K (PK) digestion assays have long been used for comparative structural analyses of amyloid oligomers and fibrils.[38, 39] The enzymatic digestion pattern of the two α-synuclein filaments was analyzed to compare their molecular structural features (Figure 5c). The PK digestion analyses revealed that the G51D filaments are cleaved more effectively than the WT α-synuclein filaments. These results suggest that the core region of the WT α-synuclein filaments is more protected from digestion than that of the G51D filaments. The structural difference was also observed in the PK digestion analyses of WT and G51D α-synuclein fibrils formed in the absence of lipid vesicles, which revealed that the G51D α-synuclein fibrils are digested more readily than the WT fibrils.[8] In addition, the G51D fibrils were shown to be more toxic to the cells than the WT fibrils.[8, 40] Our toxicity assay using MTT also showed that the DMPS-derived G51D filaments exhibit stronger cytotoxicity than the DMPS-derived WT filaments (Figure 5d), as was observed for the α-synuclein fibrils formed in the absence of lipid vesicles.

Discussion

Recent advances in cryo-EM and solid-state NMR methodologies enabled the structural determination of amyloid filaments at atomic resolution.[2–6] The high-resolution structural studies revealed that α-synuclein can form diverse filamentous aggregates with different molecular conformations under different buffer conditions. In addition, ex vivo α-synuclein filaments extracted from MSA and DLB patients' brains were shown to adopt distinct molecular conformations from those of the in vitro filaments.[11, 12] In particular, only untwisted filamentous aggregates were observed for the extracts from DLB patients. These results suggest the presence of co-factors involved in the formation of α-synuclein filaments in vivo.

Aggregation of α-synuclein is affected by a variety of factors such as metal ions, negatively charged lipids, other aggregation-prone proteins including tau, and DNA.[19, 41–43] Cofactors in different cellular environments may play an important role in promoting misfolding and aggregation of α-synuclein in vivo.[18] It was also previously suggested that α-synuclein interacts with synaptic vesicle membranes in dopaminergic neurons.[23, 24] In addition, co-localization of lipid membranes and α-synuclein aggregates in LB[28] suggests a critical role of lipid membranes in misfolding and aggregation of α-synuclein.[44]

Model membrane vesicles consisting of DMPS have been used to explore the effect of the lipid vesicles on α-synuclein aggregation and morphology of α-synuclein aggregates.[19, 27, 36] In this study, cryo-EM was used to investigate structural features of α-synuclein aggregates formed in the presence of DMPS vesicles. Our structural analyses revealed that the DMPS-induced α-synuclein filaments adopt untwisted conformations with a diameter of 5 – 13 nm, which are drastically from those of the in vitro twisted α-synuclein fibrils formed in the absence of DMPS[8]. The untwisted filaments are rather similar to those observed in brain extracts from DLB patients. The anionic lipids were shown to interact with the N-terminal region of α-synuclein,[45] which may disrupt long-range interactions between the N- and C-terminal regions and accelerate the formation of fibrils[46, 47]. The interactions between the N-terminal region of α-synuclein and anionic lipids may also lead the protein to an aggregation pathway toward untwisted filaments. On the contrary, our previous structural studies showed that an aggregation-prone protein, tau, interacts with the C-terminal region of α-synuclein, promoting the formation of twisted fibrils with distinct molecular conformations.[14, 15] These results suggest that interactions between cofactors and α-synuclein may lead to the formation of diverse α-synuclein fibrils.[48]

A series of large helical fibrils with diameters of 40 – 100 nm reported in a previous structural study (100 μM of WT α-synuclein with 200 μM of DMPS vesicles with a diameter of 20 nm at pH 6.5)[27] are, however, not detected in our experimental conditions (60 μM of G51D α-synuclein with 100 μM of DMPS vesicles with a diameter of 70 nm at pH 7.4). In addition, a very recent structural study demonstrated that phospholipid vesicles consisting of POPC/POPA (1:1, lipid to protein ratio of 5:1) induced the formation of twisted WT α-synuclein filaments of 10 – 15 nm in thickness with a helical pitch of 90 – 120 nm.[49] These results indicate that the morphology of α-synuclein filaments derived by lipid vesicles depends on the lipid composition, protein to lipid ratio, size of the

vesicles, and the mutation that may modulate α-synuclein bindings[21, 50]. Further studies are, therefore, needed to investigate the effect of those factors on the filament structure.

Atomic-resolution structure of the DMPS-derived G51D filaments could not be determined since only one orientation was available in the cryo-images. In addition, the curly DMPS-derived WT filaments were not amenable for cryo-EM structural studies. Thus, the structural, and biochemical properties of the two DMPS-derived filaments were compared with commonly used biophysical and biochemical techniques. Structural analyses using CD spectroscopy revealed that the two α-synuclein filaments have similar secondary structural features with similar ThT binding affinities and seeding properties. The two DMPS-induced filaments exhibit distinct CD spectra from those of more α-structured twisted fibrils formed in the absence of DMPS vesicles, suggesting that WT α-synuclein may also form untwisted conformations. The more flexible, curly morphology of the DMPS-induced WT and G51D α-synuclein filaments may also originate from the untwisted structures.

It is also notable that the DMPS-derived G51D filaments were more effectively digested by the PK enzyme than the DMPS-derived WT filaments. In addition, the G51D filaments exhibited stronger cytotoxic activities than the WT filaments. Similar trends were observed in previous biochemical studies for the WT and G51D fibrils formed in the absence of lipid vesicles.[8, 40] Cryo-EM structural studies revealed that the WT and mutant fibrils adopt similar molecular conformations of the fibril core region consisting of residues 60 – 98 (Figure S7).[8] The single-point mutation, however, disrupts the interfacial region (residues 50 – 57) of the WT fibrils, and the interfacial segment with residue 51 unfolds and forms β-hairpin with the other segment (residues 50 – 67) in the G51D fibrils (Figure S7b). The structural rearrangement yields more extended, less compact fibril core in the G51D fibrils, which might be more amenable for PK digestion. Although the effect of the G51D mutation on the DMPS-derived filaments is not clear because the atomic structure of the DMPS-derived filaments is not available, similar trends in the PK digestion and cytotoxicity assays suggest that the G51D mutation may partly disrupt the core region of the WT filaments, leading to less compact core structures that are more accessible to the digestive enzymes.

In summary, we report untwisted straight filaments with diameters of 5 – 13 nm formed in the presence of DMPS lipid vesicles, which have not been previously observed for in vitro α-synuclein aggregates. The untwisted straight filaments are morphologically similar to those extracted from DLB patients, suggesting that lipid vesicles may play an important role in α-synuclein aggregation in vivo. The new structures induced by the lipid vesicles also imply that interactions between α-synuclein and cofactors may lead the protein to distinct misfolding and aggregation pathways, highlighting the important role of cofactors in cellular environments.

Supplementary Material

Refer to Web version on PubMed Central for supplementary material.

Funding Sources

This work was supported in part by NIH R01 NS097490 (K.H.L.), R01 AG054025 (R.K.), R01 NS094557 (R.K.), R35 GM139616 (K.A.T.) and by Intramural Research Program of the NIH; National Institute of Environmental Health Sciences Grant ZIC ES103326 (M.J.B.).

ABBREVIATIONS

PD	Parkinson’s disease
DMPS	1,2-dimyristoyl-sn-glycero-3-phospho-L-serine
TEM	transmission electron microscopy
DARR	dipolar assisted rotational resonance
cryo-EM	cryo-electron microscopy
MSA	multiple system atrophy
DLB	dementia with Lewy bodies
ThT	thioflavin T
DLS	Dynamic light scattering
CTF	contrast transfer function
POPA	1-palmitoyl-2-oleoyl-*sn*-glycero-3-phosphate
PK	proteinase K
POPC	1-palmitoyl-2-oleoyl-*sn*-glycero-3-phosphocholine
ANS	8-anilino-1-naphthalenesulfonic acid
MTT	3-(4,5-dimethylthiazol-2-yl)-2,5-diphenyltetrazolium bromide

References

1. Goedert M (2001) Alpha-synuclein and neurodegenerative diseases. Nat. Rev. Neurosci 2, 492–501. [PubMed: 11433374]
2. Guerrero-Ferreira R, Taylor NM, Mona D, Ringler P, Lauer ME, Riek R, Britschgi M, and Stahlberg H (2018) Cryo-EM structure of alpha-synuclein fibrils. Elife. 7, 10.7554/eLife.36402.
3. Li Y, Zhao C, Luo F, Liu Z, Gui X, Luo Z, Zhang X, Li D, Liu C, and Li X (2018) Amyloid fibril structure of alpha-synuclein determined by cryo-electron microscopy. Cell Res. 28, 897–903. [PubMed: 30065316]
4. Li B, Ge P, Murray KA, Sheth P, Zhang M, Nair G, Sawaya MR, Shin WS, Boyer DR, Ye S, Eisenberg DS, Zhou ZH, and Jiang L (2018) Cryo-EM of full-length alpha-synuclein reveals fibril polymorphs with a common structural kernel. Nat. Commun 9, 3609–2. [PubMed: 30190461]
5. Ni X, McGlinchey RP, Jiang J, and Lee JC (2019) Structural insights into α-synuclein fibril polymorphism: Effects of parkinson’s disease-related C-terminal truncations. J. Mol. Biol 431, 3913–3919. [PubMed: 31295458]
6. Tuttle MD, Comellas G, Nieuwkoop AJ, Covell DJ, Berthold DA, Kloepper KD, Courtney JM, Kim JK, Barclay AM, Kendall A, Wan W, Stubbs G, Schwieters CD, Lee VM, George JM, and Rienstra

CM (2016) Solid-state NMR structure of a pathogenic fibril of full-length human alpha-synuclein. Nat. Struct. Mol. Biol 23, 409–415. [PubMed: 27018801]

7. Boyer DR, Li B, Sun C, Fan W, Zhou K, Hughes MP, Sawaya MR, Jiang L, and Eisenberg DS (2020) The α-synuclein hereditary mutation E46K unlocks a more stable, pathogenic fibril structure. Proc. Natl. Acad. Sci. U. S. A 117, 3592–3602. [PubMed: 32015135]
8. Sun Y, Long H, Xia W, Wang K, Zhang X, Sun B, Cao Q, Zhang Y, Dai B, Li D, and Liu C (2021) The hereditary mutation G51D unlocks a distinct fibril strain transmissible to wild-type α-synuclein. Nat. Commun 12, 6252–2. [PubMed: 34716315]
9. Boyer DR, Li B, Sun C, Fan W, Sawaya MR, Jiang L, and Eisenberg DS (2019) Structures of fibrils formed by α-synuclein hereditary disease mutant H50Q reveal new polymorphs. Nat. Struct. Mol. Biol 26, 1044–1052. [PubMed: 31695184]
10. Sun Y, Hou S, Zhao K, Long H, Liu Z, Gao J, Zhang Y, Su XD, Li D, and Liu C (2020) Cryo-EM structure of full-length α-synuclein amyloid fibril with parkinson's disease familial A53T mutation. Cell Res. 30, 360–362. [PubMed: 32203130]
11. Schweighauser M, Shi Y, Tarutani A, Kametani F, Murzin AG, Ghetti B, Matsubara T, Tomita T, Ando T, Hasegawa K, Murayama S, Yoshida M, Hasegawa M, Scheres SHW, and Goedert M (2020) Structures of α-synuclein filaments from multiple system atrophy. Nature. 585, 464–469. [PubMed: 32461689]
12. Van der Perren A, Gelders G, Fenyi A, Bousset L, Brito F, Peelaerts W, Van den Haute C, Gentleman S, Melki R, and Baekelandt V (2020) The structural differences between patient-derived α-synuclein strains dictate characteristics of parkinson's disease, multiple system atrophy and dementia with lewy bodies. Acta Neuropathol. 139, 977–1000. [PubMed: 32356200]
13. Guerrero-Ferreira R, Kovacik L, Ni D, and Stahlberg H (2020) New insights on the structure of alpha-synuclein fibrils using cryo-electron microscopy. Curr. Opin. Neurobiol 61, 89–95. [PubMed: 32112991]
14. Dasari AKR, Kayed R, Wi S, and Lim KH (2019) Tau interacts with the C-terminal region of α-synuclein, promoting formation of toxic aggregates with distinct molecular conformations. Biochemistry. 58, 2814–2821. [PubMed: 31132261]
15. Hojjatian A, Dasari AKR, Sengupta U, Taylor D, Daneshparvar N, Yeganeh FA, Dillard L, Michael B, Griffin RG, Borgnia MJ, Kayed R, Taylor KA, and Lim KH (2021) Tau induces formation of α-synuclein filaments with distinct molecular conformations. Biochem. Biophys. Res. Commun 554, 145–150. [PubMed: 33798940]
16. Comellas G, Lemkau LR, Zhou DH, George JM, and Rienstra CM (2012) Structural intermediates during α-synuclein fibrillogenesis on phospholipid vesicles. J. Am. Chem. Soc 134, 5090–5099. [PubMed: 22352310]
17. Candelise N, Schmitz M, Thüne K, Cramm M, Rabano A, Zafar S, Stoops E, Vanderstichele H, Villar-Pique A, Llorens F, and Zerr I (2020) Effect of the micro-environment on α-synuclein conversion and implication in seeded conversion assays. Transl. Neurodegener 9, 5–9. eCollection 2020. [PubMed: 31988747]
18. Peng C, Gathagan RJ, Covell DJ, Medellin C, Stieber A, Robinson JL, Zhang B, Pitkin RM, Olufemi MF, Luk KC, Trojanowski JQ, and Lee VM (2018) Cellular milieu imparts distinct pathological alpha-synuclein strains in alpha-synucleinopathies. Nature. 557, 558–563. [PubMed: 29743672]
19. Galvagnion C, Buell AK, Meisl G, Michaels TC, Vendruscolo M, Knowles TP, and Dobson CM (2015) Lipid vesicles trigger α-synuclein aggregation by stimulating primary nucleation. Nat. Chem. Biol 11, 229–234. [PubMed: 25643172]
20. Kiechle M, Grozdanov V, and Danzer KM (2020) The role of lipids in the initiation of α-synuclein misfolding. Front. Cell. Dev. Biol 8, 562241. [PubMed: 33042996]
21. Pfefferkorn CM, Jiang Z, and Lee JC (2012) Biophysics of α-synuclein membrane interactions. Biochim. Biophys. Acta 1818, 162–171. [PubMed: 21819966]
22. Auluck PK, Caraveo G, and Lindquist S (2010) A-synuclein: Membrane interactions and toxicity in parkinson's disease. Annu. Rev. Cell Dev. Biol 26, 211–233. [PubMed: 20500090]

23. Shibayama-Imazu T, Okahashi I, Omata K, Nakajo S, Ochiai H, Nakai Y, Hama T, Nakamura Y, and Nakaya K (1993) Cell and tissue distribution and developmental change of neuron specific 14 kDa protein (phosphoneuroprotein 14). Brain Res. 622, 17–25. [PubMed: 7694766]
24. Maroteaux L, Campanelli JT, and Scheller RH (1988) Synuclein: A neuron-specific protein localized to the nucleus and presynaptic nerve terminal. J. Neurosci 8, 2804–2815. [PubMed: 3411354]
25. Galvagnion C (2017) The role of lipids interacting with α-synuclein in the pathogenesis of parkinson's disease. Journal of Parkinson's Disease. 7, 433–450.
26. Brown JWP, Meisl G, Knowles TPJ, Buell AK, Dobson CM, and Galvagnion C (2018) Kinetic barriers to α-synuclein protofilament formation and conversion into mature fibrils. Chem. Commun. (Camb) 54, 7854–7857. [PubMed: 29951679]
27. Meade RM, Williams RJ, and Mason JM (2020) A series of helical α-synuclein fibril polymorphs are populated in the presence of lipid vesicles. NPJ Parkinsons Dis. 6, 17–1. eCollection 2020. [PubMed: 32864427]
28. Shahmoradian SH, Lewis AJ, Genoud C, Hench J, Moors TE, Navarro PP, Castaño-Díez D, Schweighauser G, Graff-Meyer A, Goldie KN, Sütterlin R, Huisman E, Ingrassia A, Gier Y, Rozemuller AJM, Wang J, Paepe A, Erny J, Staempfli A, Hoernschemeyer J, Großerüschkamp F, Niedieker D, El-Mashtoly SF, Quadri M, Van IJcken WFJ, Bonifati V, Gerwert K, Bohrmann B, Frank S, Britschgi M, Stahlberg H, Van de Berg WDJ, and Lauer ME (2019) Lewy pathology in parkinson's disease consists of crowded organelles and lipid membranes. Nat. Neurosci 22, 1099–1109. [PubMed: 31235907]
29. Kiely AP, Ling H, Asi YT, Kara E, Proukakis C, Schapira AH, Morris HR, Roberts HC, Lubbe S, Limousin P, Lewis PA, Lees AJ, Quinn N, Hardy J, Love S, Revesz T, Houlden H, and Holton JL (2015) Distinct clinical and neuropathological features of G51D SNCA mutation cases compared with SNCA duplication and H50Q mutation. Molecular Neurodegeneration. 10, 41. [PubMed: 26306801]
30. Kiechle M, Grozdanov V, and Danzer KM (2020) The role of lipids in the initiation of α-synuclein misfolding. Frontiers in Cell and Developmental Biology. 8. 1–9. [PubMed: 32117956]
31. Sinning A, and Hübner CA (2013) Minireview: pH and synaptic transmission. FEBS Lett. 587, 1923–1928. [PubMed: 23669358]
32. Ghee M, Melki R, Michot N, and Mallet J (2005) PA700, the regulatory complex of the 26S proteasome, interferes with alpha-synuclein assembly. FEBS J 272, 4023–4033. [PubMed: 16098186]
33. Zheng SQ, Palovcak E, Armache JP, Verba KA, Cheng Y, and Agard DA (2017) MotionCor2: Anisotropic correction of beam-induced motion for improved cryo-electron microscopy. Nat. Methods 14, 331–332. [PubMed: 28250466]
34. Zhang K (2016) Gctf: Real-time CTF determination and correction. J. Struct. Biol 193, 1–12. [PubMed: 26592709]
35. Zivanov J, Nakane T, Forsberg BO, Kimanius D, Hagen WJ, Lindahl E, and Scheres SH (2018) New tools for automated high-resolution cryo-EM structure determination in RELION-3. Elife. 7, 10.7554/eLife.42166.
36. Flagmeier P, Meisl G, Vendruscolo M, Knowles TP, Dobson CM, Buell AK, and Galvagnion C (2016) Mutations associated with familial parkinson's disease alter the initiation and amplification steps of α-synuclein aggregation. Proc. Natl. Acad. Sci. U. S. A 113, 10328–10333. [PubMed: 27573854]
37. Spillantini MG, Crowther RA, Jakes R, Cairns NJ, Lantos PL, and Goedert M (1998) Filamentous alpha-synuclein inclusions link multiple system atrophy with parkinson's disease and dementia with lewy bodies. Neurosci. Lett 251, 205–208. [PubMed: 9726379]
38. Collinge J, Sidle KC, Meads J, Ironside J, and Hill AF (1996) Molecular analysis of prion strain variation and the aetiology of 'new variant' CJD. Nature. 383, 685–690. [PubMed: 8878476]
39. Bousset L, Pieri L, Ruiz-Arlandis G, Gath J, Jensen PH, Habenstein B, Madiona K, Olieric V, Böckmann A, Meier BH, and Melki R (2013) Structural and functional characterization of two alpha-synuclein strains. Nat. Commun 4, 2575. [PubMed: 24108358]

40. Hayakawa H, Nakatani R, Ikenaka K, Aguirre C, Choong CJ, Tsuda H, Nagano S, Koike M, Ikeuchi T, Hasegawa M, Papa SM, Nagai Y, Mochizuki H, and Baba K (2020) Structurally distinct α-synuclein fibrils induce robust parkinsonian pathology. Mov. Disord 35, 256–267. [PubMed: 31643109]
41. Stephens AD, Zacharopoulou M, and Kaminski Schierle GS (2019) The cellular environment affects monomeric α-synuclein structure. Trends Biochem. Sci 44, 453–466. [PubMed: 30527975]
42. Giasson BI, Forman MS, Higuchi M, Golbe LI, Graves CL, Kotzbauer PT, Trojanowski JQ, and Lee VM (2003) Initiation and synergistic fibrillization of tau and alpha-synuclein. Science. 300, 636–640. [PubMed: 12714745]
43. Sengupta U, Puangmalai N, Bhatt N, Garcia S, Zhao Y, and Kayed R (2020) Polymorphic α-synuclein strains modified by dopamine and docosahexaenoic acid interact differentially with tau protein. Mol. Neurobiol 57, 2741–2765. [PubMed: 32350746]
44. Dikiy I, and Eliezer D (2012) Folding and misfolding of alpha-synuclein on membranes. Biochim. Biophys. Acta 1818, 1013–1018. [PubMed: 21945884]
45. Trexler AJ, and Rhoades E (2009) Alpha-synuclein binds large unilamellar vesicles as an extended helix. Biochemistry. 48, 2304–2306. [PubMed: 19220042]
46. Dedmon MM, Lindorff-Larsen K, Christodoulou J, Vendruscolo M, and Dobson CM (2005) Mapping long-range interactions in alpha-synuclein using spin-label NMR and ensemble molecular dynamics simulations. J. Am. Chem. Soc 127, 476–477. [PubMed: 15643843]
47. Bertoncini CW, Jung YS, Fernandez CO, Hoyer W, Griesinger C, Jovin TM, and Zweckstetter M (2005) Release of long-range tertiary interactions potentiates aggregation of natively unstructured alpha-synuclein. Proc. Natl. Acad. Sci. USA 102, 1430–1435. [PubMed: 15671169]
48. Kim C, Lv G, Lee JS, Jung BC, Masuda-Suzukake M, Hong CS, Valera E, Lee HJ, Paik SR, Hasegawa M, Masliah E, Eliezer D, and Lee SJ (2016) Exposure to bacterial endotoxin generates a distinct strain of alpha-synuclein fibril. Sci. Rep 6, 30891. [PubMed: 27488222]
49. Antonschmidt L, Dervişoğlu R, Sant V, Tekwani Movellan K, Mey I, Riedel D, Steinem C, Becker S, Andreas LB, and Griesinger C (2021) Insights into the molecular mechanism of amyloid filament formation: Segmental folding of α-synuclein on lipid membranes. Sci. Adv 7, eabg2174. doi: 10.1126/sciadv.abg2174. Print 2021 May.
50. Middleton ER, and Rhoades E (2010) Effects of curvature and composition on α-synuclein binding to lipid vesicles. Biophys. J 99, 2279–2288. [PubMed: 20923663]

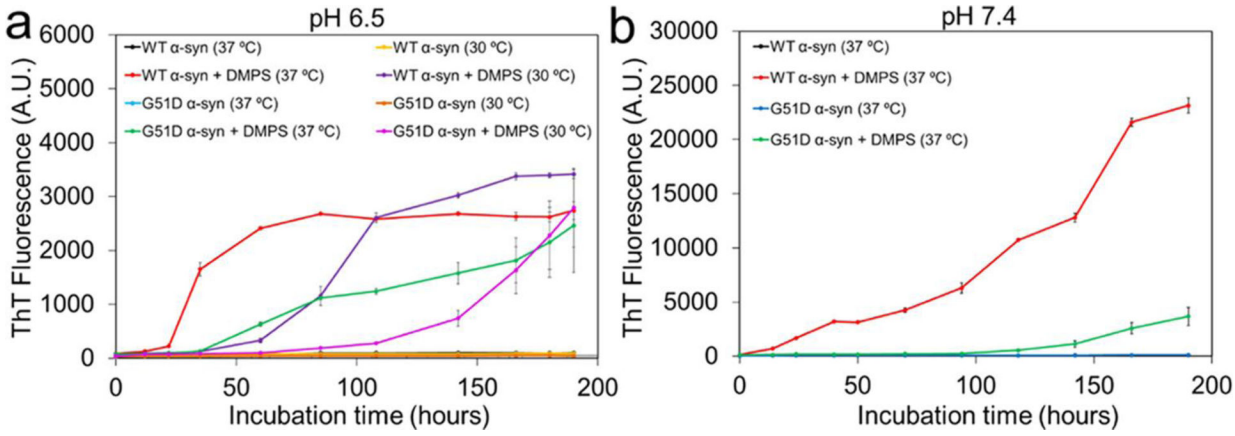

Figure 1:

Aggregation kinetics of α-synuclein (60 μM) in the absence and presence of the DMPS SUVs (100 μM) at pH 6.5 (a) and pH 7.4 (b) under the quiescent condition. ThT fluorescence of all of the α-synuclein samples in the absence of the DMPS vesicles was nearly zero at the incubation periods.

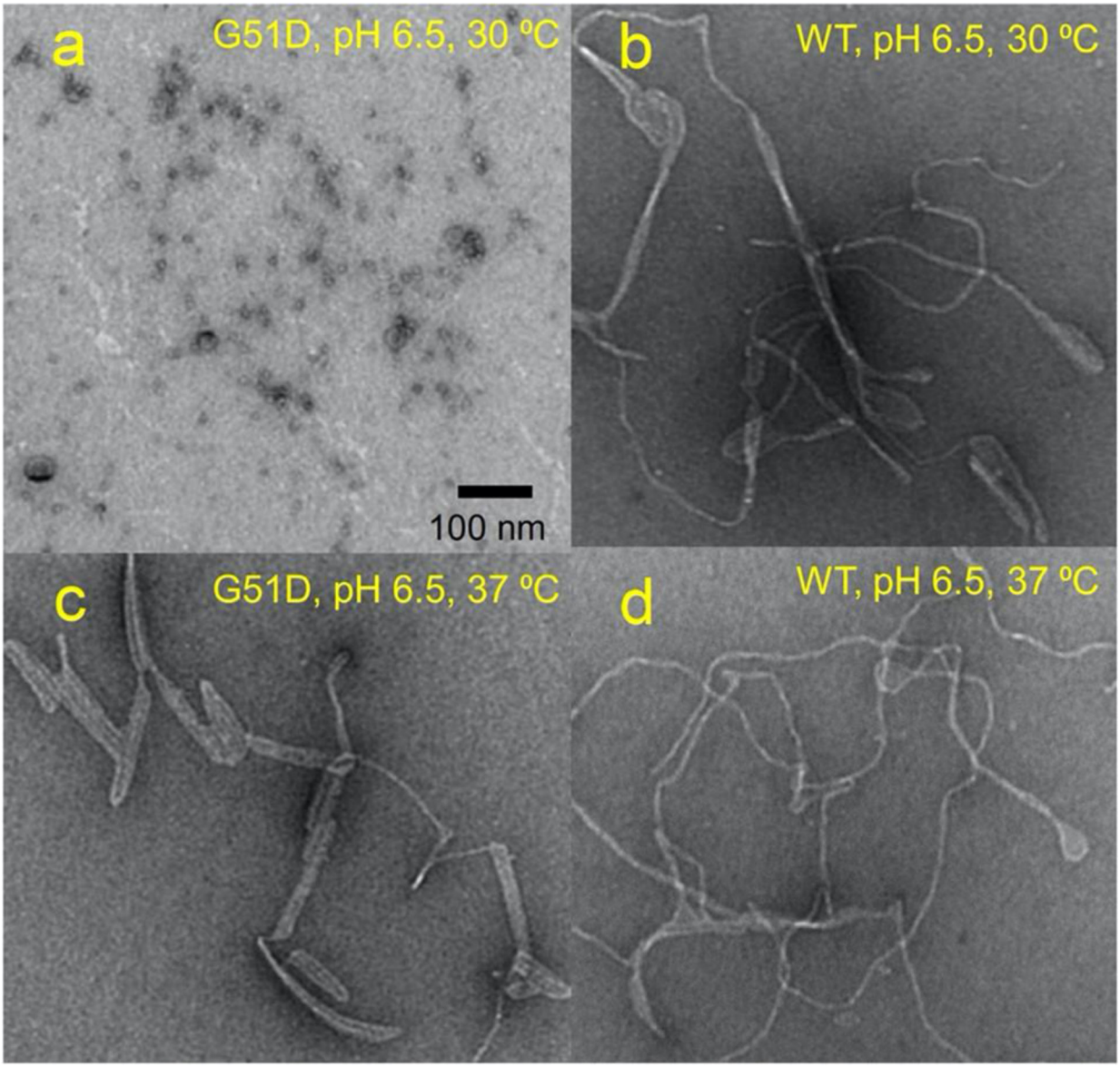

Figure 2:

TEM images of G51D α-synuclein at pH 6.5 and 30 °C (a), WT α-synuclein at pH 6.5 and 30 °C (b), G51D α-synuclein at pH 6.5 and 37 °C (c), and WT α-synuclein at pH 6.5 and 37 °C (d). Protein samples (60 μM) were incubated for 7 days in the presence of DMPS (100 μM) lipid vesicles of an average diameter of 70 nm. No filaments were observed in the absence of the lipid vesicles.

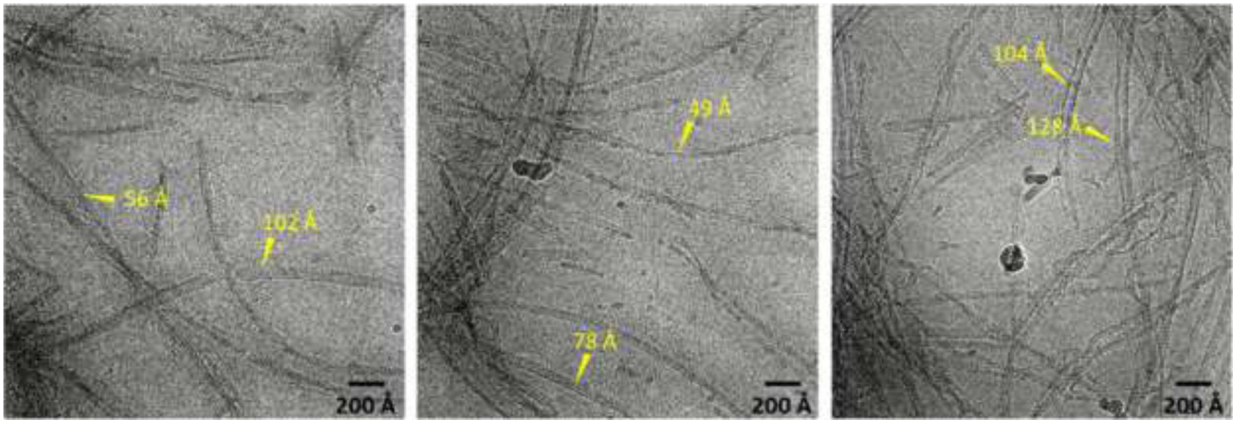

Figure 3:

Representative cryo-EM micrographs of G51D α-synuclein (60 μM) incubated for 30 days in the presence of DMPS (100 μM) vesicles with an average diameter of 70 nm.

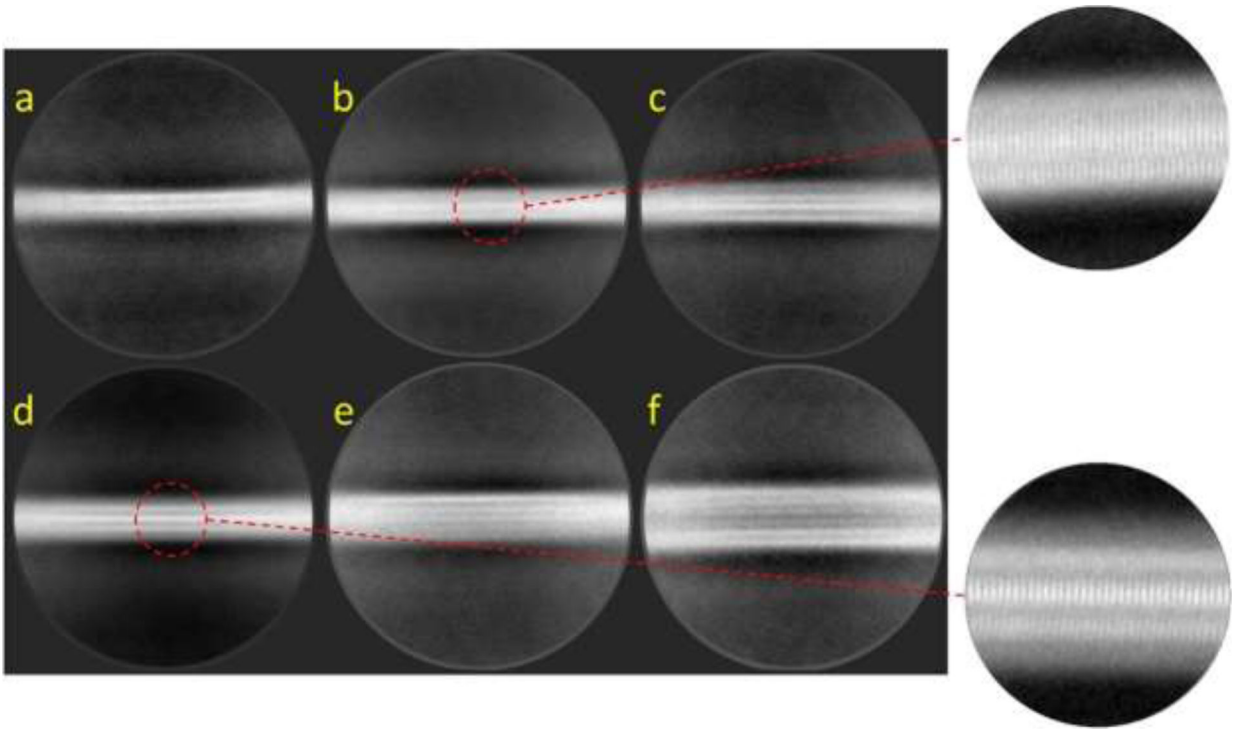

Figure 4:

(a–f) Representative reference-free 2D class averages of G51D α-synuclein filaments formed in the presence of DMPS SUVs were obtained with a box size of 56 nm.

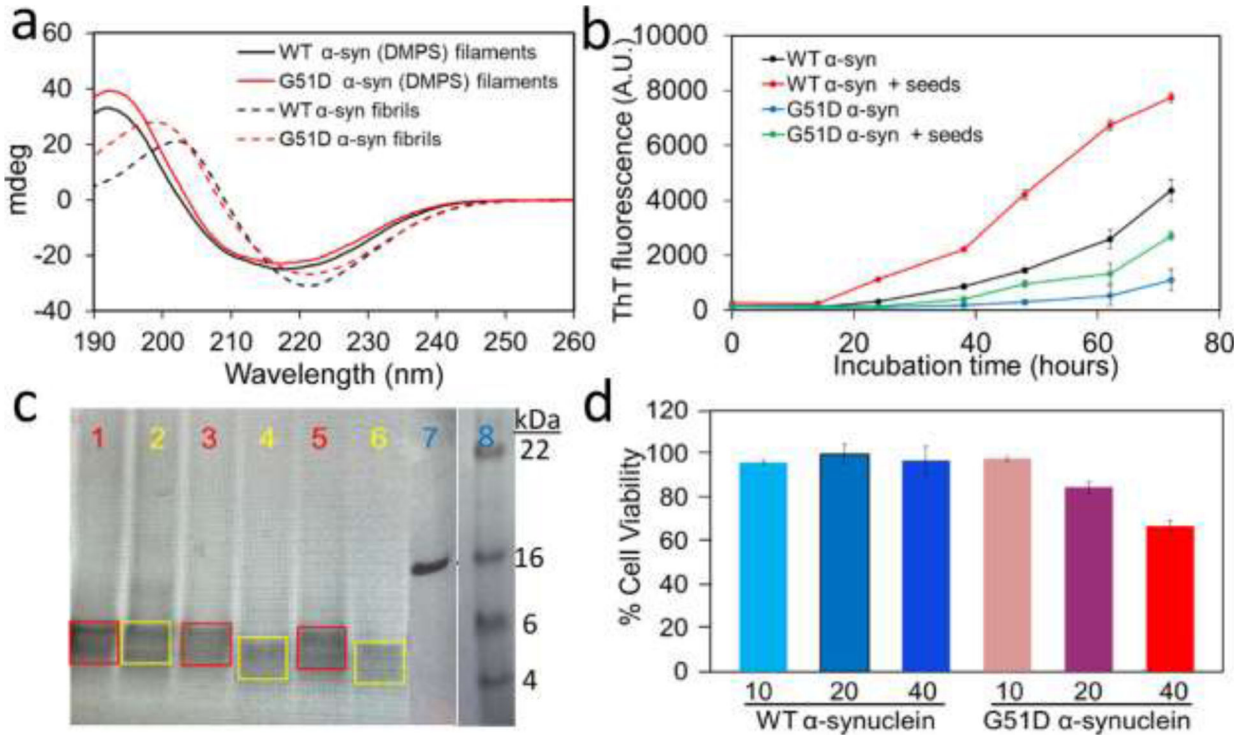

Figure 5:

(a) CD spectra of α-synuclein filaments (solid lines) and fibrils (dotted lines) formed in the presence and absence of DMPS lipids, respectively. CD spectra of the DMPS-derived WT and G51D α-synuclein (10 μM) were measured using a 1 mm pathlength quartz cuvette on a Jasco 815 spectrometer. (b) Aggregation kinetics of WT and G51D α-synuclein (60 μM) seeded with the DMPS-derived α-synuclein filaments (0.6 μM) in the presence of ThT at 37 °C under constant agitation at 250 rpm. Aggregation kinetics were monitored by measuring ThT fluorescence with excitation and emission wavelengths of 440 and 482 nm, respectively. (c) Proteinase K digestion analyses of DMPS-derived WT (red) and G51D (yellow) α-synuclein filaments. α-Synuclein filaments (14 μM) were mixed with proteinase K (0.5 ng/μL) and incubated for 1 min (bands 1 and 2), 10 min (bands 3 and 4), and 20 min (bands 5 and 6). The core bands after the digestion are marked in red (WT) and yellow (G51D). Bands 7 and 8 are the α-synuclein monomer and the protein ladder, respectively. Protein samples were run on 4–12% SDS-PAGE gel. (d) MTT cell viability assay for the DMPS-derived WT and G51D α-synuclein filaments at 10, 20, and 40 μM monomeric concentrations.